Journal of Applied Physics ARTICLE scitation.org/journal/jap

# Density-functional theory calculation of magnetic properties of $BiFeO_3$ and $BiCrO_3$ under epitaxial strain

Cite as: J. Appl. Phys. **130**, 104102 (2021); doi: 10.1063/5.0054979
Submitted: 23 April 2021 · Accepted: 20 August 2021 ·
Published Online: 14 September 2021



Michael R. Walden,[1,a)] Cristian V. Ciobanu,[2] and Geoff L. Brennecka[1]

## AFFILIATIONS

[1]Department of Metallurgical and Materials Engineering, Colorado School of Mines, Golden, Colorado 80401, USA
[2]Department of Mechanical Engineering, Colorado School of Mines, Golden, Colorado 80401, USA

[a)]**Author to whom correspondence should be addressed:** waldenmichael@mines.edu

## ABSTRACT

This work uses density-functional theory to model the magnetic properties of bismuth-based perovskite oxides under epitaxial strain. We augment the known transition in $BiFeO_3$ between rhombohedral-like and tetragonal-like phases occurring at 4.2% compressive epitaxial strain with the variation in magnetic behavior near this boundary. This phase boundary coincides with a transition from G- to C-type magnetic order, as well as with a 90% decrease in the magnitude of the [001]-oriented coupling coefficients. The magnitude of iron magnetization is shown to vary by no more than 3% over the entire range of compressive strain considered. In the $BiCrO_3$ system, we report a variation in chromium magnetization of over 20%, along with transitions from bulk G-type to regions of C-type order under tensile epitaxial strain and to F-type order under both tensile and compressive epitaxial strains. The region of F-type order stabilized under compression beyond 7.9% epitaxial strain corresponds to a "super-tetragonal" phase structurally similar to the well-known phase of $BiFeO_3$ exhibiting spontaneous polarization on the order of 150 $\mu C/cm^2$.



## I. INTRODUCTION

The bismuth-based perovskite oxides are a series of materials frequently exhibiting ferroelectric and ferromagnetic orders.[1–9] The members of this series share the generic chemical formula $BiXO_3$ or $BXO$, where $X$ corresponds to one or more trivalent cations, most commonly Cr, Mn, Fe, Ni, or Co. Aside from the $BiFeO_3$ (BFO) system, phase stability and magnetic properties in these systems remain underexplored, though the quantitative characteristics of antiferromagnetic (AFM) response in the BFO system under epitaxial strain also require further investigation.[7–12] In addition to providing a computational investigation of assessment of magnetic response in the BFO system to epitaxial strain, this work identifies the extent to which another noteworthy BXO system, $BiCrO_3$ (BCO), also exhibits useful variation in structural and magnetic order under epitaxial strain.

Epitaxial strain provides a mechanism in the multiferroic $BXO$ systems for the stabilization of structural order or magnetic order, which may be unstable in a bulk context. A commonly reported example of such an enhancement of ferroic response is the stabilization under approximately 6% compressive epitaxial strain of a "super-tetragonal" phase of BFO having very high spontaneous polarization on the order of 150 $\mu C/cm^2$.[2] In addition, transitions in the BFO system from G-type to C-type magnetic order have been reported under compressive epitaxial strain.[13,14] The rhombohedral-like and super-tetragonal structural configurations of BFO are illustrated in Fig. 1, along with all four magnetic orders compatible with magnetic coupling exclusively between first-neighboring B-site cations. While the quantitative characteristics of the transition in structural order in the BFO system have been systematically investigated using *ab initio* techniques in the existing literature, a robust computational investigation of magnetic behavior under epitaxial strain has not been undertaken. Additionally, systematic investigations neither of structural nor of magnetic order under epitaxial strain in the BCO system exist to our knowledge, aside from our own investigation of structural order in the BCO system.[12]

There are many approaches to modeling phase stability and magnetic order under epitaxial strain from first-principles.

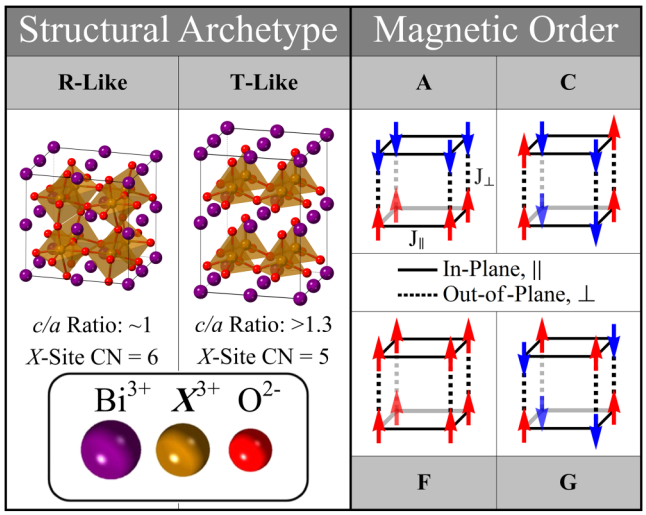


**FIG. 1.** Structural archetypes and first-neighbor magnetic orders associated with the BXO material systems. Oxygen coordination illustrated as octahedra (coordination number, CN = 6) and lower-coordination polyhedra (CN = 5) in the R-like and T-like archetypes, respectively.

Modeling space group stability under epitaxial strain requires selective relaxation of lattice parameters, in which a given condition of epitaxial strain must be "frozen" in the computational scheme while allowing the remaining lattice parameters to relax to their lowest-energy values. Examples of approximate relaxation schemes include considering a supercell by symmetry disallowing space groups other than *Cc* monoclinic or *P4mm*, relaxing either the in-plane lattice constant or the $c/a$ ratio, or freezing the pseudocubic lattice angle 90°.[15–18] Many structural investigations of BFO epitaxial phase stability assume uniformly G-type antiferromagnetic order, and as such do not consider variation in magnetic coupling with strain.[12,16,18]

Modeling magnetic order subject to a classical Heisenberg-like Hamiltonian may ignore variation in the magnetic moment, calculating the $J_{i,j}$ coupling coefficients directly as differences in the energy of different magnetic orders.[13,14] In this article, we use density-functional theory (DFT) calculations to determine both the magnetic moments and magnetic coupling coefficients for a Heisenberg-like model of the B-site lattice in perovskite films subjected to epitaxial strain. Calculation of magnetic coupling coefficients in a Heisenberg-like model may consider only first nearest-neighboring B-site pairs or second neighbors as well. The predominant basis for magnetic ordering in the BXO systems is a superexchange mechanism, in which B-site coupling is mediated by the oxygen anion intermediate between two first-neighboring B-site cations.[19] Because second-neighboring B-site cations do not have an intermediate oxygen anion, only the coupling of first-neighboring B-sites is considered in our calculations. Those computational works which consider second-neighbor coupling coefficients (by raw differences in energy with no consideration of variation in the moment) find a uniform magnitude of this coefficient across the full range of epitaxial strain. This behavior is functionally equivalent to a uniform energy offset from sole consideration of first nearest-neighbor coupling.[13]

Our previous work has shown that, of the BXO series with B-site occupation by a trivalent cation from among the 3d metals, the BFO and BCO systems are the lone systems exhibiting two or more stable space groups and/or magnetic orders under epitaxial strain.[12] The relevant crystallographic classes include monoclinic, triclinic, and tetragonal space groups for BFO, and monoclinic and orthorhombic space groups for BCO. These structural configurations may be categorized as rhombohedral-like (R-like) or tetragonal-like (T-like), per the illustrations in Fig. 1, depending on the structural similarity of the stable phase to an *R3c* or *P4mm* structural archetype.[10,11,15–18,20–27] Previous literature has shown that first-neighbor magnetic coupling accounts for translational symmetry present in the BXO systems under epitaxial strain, yielding the four (A-, C-, F-, G-type) orders associated with the various combinations of positive and negative signs on the in-plane and out-of-plane coupling coefficients, also as illustrated in Fig. 1. The combination of space group and magnetic order, such as *R3c*-G or *P4mm*-C, fully defines a "chemical phase" to which epitaxial strain will be applied in this work.[13]

The phases shown to be stable in the BFO and BCO systems correspond to several unique B-site ($XO_6$) coordination environments.[12,15–18,20–22,25] Because of the strong dependence of magnetic order on this coordination environment, there is the potential for multiple stable magnetic orders in the BFO and BCO systems.[17,19] The current work determines the extent of complexity in the magnetic response exhibited by the BFO and BCO material systems under variation of epitaxial strain, principally yielding predictions of both space group and magnetic order, which are the lowest energy for any reasonable range of compressive or tensile epitaxial strain. As a second yield, the current work identifies the variation in magnetic moments and first-neighbor magnetic coupling coefficients with epitaxial strain.

## II. METHODS

### A. Structural relaxations

We have used the Vienna *ab initio* Simulation Package (VASP)[28–31] to conduct DFT calculations in the framework of the spin-polarized generalized gradient approximation, implemented with "PBEsol" exchange-correlation functionals.[32–35] The methodology used in the current work is similar to that used in our previous work,[12] with two main differences: (a) we now use the PBEsol exchange-correlation functional, due to its greater consistency with experimentally reported values of lattice constants in the BXO systems than Perdew–Burke–Ernzerhof (PBE) and (b) we consider the four types of magnetic order (A-, C-, F-, and G-type) consistent with non-zero coupling only between first-neighboring B-site cations (Fig. 1). The valence electron configurations for the plane-wave augmented pseudopotentials[36] that we employ are as follows: $6s^2 5d^{10} 6p^3$ for Bi, $3p^6 4s^2 3d^6$ for Fe, $364s^1 3d^5$ for Cr, and $2s^2 2p^4$ for O. The supercells used in this work are only as large as is necessary to capture the four types of first-neighboring magnetic order, consistent with exact 1:1:3 stoichiometry of a $BiXO_3$ perovskite. No vacancies or other site defects are considered nor are dislocations.

The role these defects would play in stabilization of epitaxial phases, or in the coherence of a thin film to a substrate, is outside the scope of this work.

We use the generalized gradient approximation with Hubbard on-site energy terms (GGA+U),[37,38] with the Hubbard corrections of $U = 4.6$ eV for Fe and 4.8 eV for Cr as calculated via linear response theory.[39] The use of GGA+U with the linear response method permits a fully *ab initio* approach to improving the quantitative validity of predictions in DFT of bandgap and other related properties arising from localized behavior of electrons. The GGA+U approach has been shown to greatly improve quantitative validity over unmodified GGA when modeling the magnetic properties of oxide systems.[40–42] Thresholds for energy convergence of $10^{-8}$ eV for electronic steps and $10^{-6}$ eV for ionic steps were used, these small values being necessary for the BCO system where energy differences between different magnetic orders of the same space group may be as small as $10^{-4}$ eV per supercell ($10^{-6}$ eV per formula unit). The calculations use either a $\sqrt{2} \times \sqrt{2} \times 2$ or $2 \times 2 \times 2$ supercell of primitive B*X*O perovskite unit cells (see Table I in the supplementary material), $5 \times 5 \times 5$ k-point mesh, and a plane-wave energy cutoff of 540 eV.[36,43]

This work does not explicitly include a substrate and instead models a crystal subject to periodic boundary conditions under *simulated* epitaxial strain. A discrete condition of epitaxial strain is modeled by designating two lattice vectors as in-plane (IP) vectors such that the area bounded by these vectors matches the square of the desired epitaxial lattice constant. Under this IP strain constraint, which simulates the equivalent condition of epitaxial strain, energy is minimized with respect to the out-of-plane (OP) lattice constant using an "external" energy minimization protocol. This protocol consists of a series of calculations with uniform **a** and **b** (IP) lattice vectors that discretely vary the component of **c** (OP) vector, which is perpendicular to the plane of IP vectors, with each calculation freezing all lattice constants while permitting relaxation of fractional atomic coordinates. The discrete values chosen for variation in the OP component of **c** cover a sufficiently wide range to ensure the determination of the global energy minimum, due to the common presence of competing local energy minima, particularly around transitions between phases and within the strain region associated with stability of a high $c/a$-ratio phase. The ultimate determination of the global energy minimum uses a much finer mesh of discrete OP components of **c**, providing energy precision at least as great as $10^{-7}$ eV per formula unit so that the precision of the VASP calculations is not lost in this "external" minimization protocol. This procedure yields a robust determination of which phases are the lowest energy at any discrete value of epitaxial strain simulated in this work. The IP lattice constants associated with the transitions between neighboring lowest-energy phase regions are identified using polynomial fits to interpolate among the appropriate discrete energy points. These polynomial fits are included in Figs. 2 and 4 as continuous curves joining the discrete energy values.

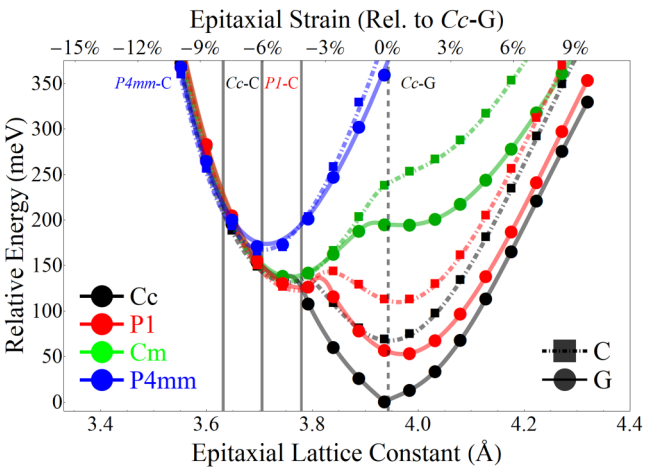


**FIG. 2.** Energetic stability of $BiFeO_3$ by *space group* and magnetic order, with strain referenced to the in-plane lattice constant ($a^* = 3.943$ Å) associated with the global minimum in the energy of the *Cc*-G phase.

## B. Determination of magnetic coupling coefficients

Once the lowest-energy combination of space group and magnetic order has been determined, the fractional ionic coordinates are frozen and the corresponding electronic configuration determined, in turn, for each of the four magnetic orders (A-, C-, F-, G-type). These calculations also yield the magnetic moment of each B-site cation. The energies and magnetic moments of each magnetic order enable the calculation of coupling coefficients based on the following equation for energy, which assumes a multiplicity of 16 and 8 for, respectively, IP and OP pairs of first-neighboring B-site cations,

$$E = E_0 + J_{\parallel} \sum_{(i,j)\in\parallel} \mu_i \mu_j + J_{\perp} \sum_{(i,j)\in\perp} \mu_i \mu_j. \quad (1)$$

In this equation, the IP and OP sets defining the ranges of the corresponding summations contain all pairs of first-neighboring IP and OP bonds within a given supercell. These summations include two IP terms and one OP term per formula unit. $E_0$ denotes the energy of a particular strain state of a given configuration of atoms, independent of magnetic order. It is necessary that the calculations of the energy of the various antiferromagnetic (AFM) order types use the same atomic configuration to avoid contributions to $E_0$ arising from lattice strain, which would conflate direct first-neighbor magnetic coupling coefficients with certain magnetoelastic coefficients. This detailed approach to calculating magnetic coupling coefficients is significantly different from other works,[44] which may simply take differences between energies of relaxed phase-order calculations, making no account for variation in the magnetic moment or for magnetoelastic effects.

In Eq. (1), each of the first-neighboring B-site moments is not presumed to have magnetic moments of the same magnitude. In order for a single IP or OP magnetic coupling coefficient to be properly associated with the entire material, it is necessary for the product of first-neighboring moments to be of uniform magnitude across all IP-neighboring B-site pairs and all OP-neighboring B-site pairs. This is a less strict condition than uniformity of

magnitude of all B-site cations. Though the global energy minimum expectation for the B*X*O systems may be antiferromagnetic order with equal moment magnitudes for all B-site cations, under sufficient epitaxial strain deviating from this ground state expectation, B-site momenta may differ in magnitude. So long as the variation in these momenta does not cause any product of adjacent IP and OP-neighboring B-site pairs to be of unequal magnitude, utilization of single IP and single OP coefficients is valid. This less strict condition, on equality of magnitudes of all neighboring moment pairs, is upheld absolutely throughout the results of this work, though no *de facto* constraint requires this outcome. For supercells in which all B-site cations have the same magnitude of the magnetic moment, Eq. (1) leads to the following equations for each magnetic order:

$$E_{X,A} = E_0 + 16J_{\parallel}\mu_{X,A}^2 - 8J_{\perp}\mu_{X,A}^2, \tag{2}$$

$$E_{X,C} = E_0 - 16J_{\parallel}\mu_{X,C}^2 + 8J_{\perp}\mu_{X,C}^2, \tag{3}$$

$$E_{X,F} = E_0 + 16J_{\parallel}\mu_{X,F}^2 + 8J_{\perp}\mu_{X,F}^2, \tag{4}$$

$$E_{X,G} = E_0 - 16J_{\parallel}\mu_{X,G}^2 - 8J_{\perp}\mu_{X,G}^2. \tag{5}$$

Because Eqs. (2)–(5) constrain only three unknown variables ($E_0$, $J_{\perp}$, $J_{\parallel}$), they yield four value predictions for each variable, thereby providing consistency checks for each predicted value. In addition, the signs of predicted coupling coefficients can be ensured to be compatible with the magnetic order, which is the lowest energy such that G-type magnetic order stability necessarily leads to IP/OP magnetic coefficients that are both positive, while A-type order stability necessitates negative IP coefficients and positive OP coefficients.

## III. RESULTS/DISCUSSION

### A. Phase stability and magnetic properties of $BiFeO_3$

The order of phases in the $BiFeO_3$ system predicted to be stable under increasing compressive epitaxial strain begins, as shown in Fig. 2, with the *Cc* space group of G-type magnetic order (described herein as the *Cc*-G phase). This space group is coincident with an *R3c* space group at 0% strain, which is consistent with previous reports that such a rhombohedral phase is the bulk (unstrained) stable phase. The lattice constant of ∼3.952 Å corresponding to this energy minimum is also highly quantitatively similar to previous reports of the global energy-minimum lattice constant of BFO. This *Cc*-G phase remains more stable than all other phases up to ∼9% tensile epitaxial strain, which is the range of tensile strain considered in this work.

Under compressive epitaxial strain, several phases transitions are predicted. The main point of agreement with the computational literature is that a "super-tetragonal" *P4mm*-C phase is stabilized under compressive strain beyond 7.9%. This phase exhibits an elongated $c/a$ ratio of at least 1.4, with potential for greatly enhanced spontaneous polarization. The intermediate region of phase stability, between 4.2% and 7.9% epitaxial strain, is found to exhibit both *Cc*-C and *P*1-C regions of phase stability. The *Cc* aspect is in agreement with the literature, but the determination of a true-triclinic *P*1 phase is not. Though previous reports have described unstable triclinic phases within this regime, the entire region of phase stability has been described as *Cc* in nature.[45] This work has definitively determined that within the 4.2%–6.0% compressive strain region, the *Cc* space group is unstable by at least $10^{-4}$ eV/$f.u.$, and the lowest-energy *P1* space group cannot be construed as a higher-symmetry space group (monoclinic or otherwise) within any reasonable thresholds. Some previous computational investigations, including a previous phase of this work, have reported stability of a *Cm* space group in some portion or all of the 4.2%–7.9% region of strain. In this work, however, the *Cm* space group is found to be energetically unstable by at least $10^{-4}$ eV/$f.u.$ for this region of strain.

It must be noted that this work and most of the extant computational literature on epitaxial phase stability in BFO exclusively consider single-phase stability. Some experimental investigations of phase stability in the 4.2%–7.9% region of compressive strain in the BFO system report some regime of stability of a mixture of two or more phases. These mixtures may include two or more monoclinic phases, or a monoclinic and tetragonal-like phase.[16,21] All mixtures are of two or more tetragonal-like phases. To our knowledge, none of these multi-phase reports include specific reference to a *P*1 triclinic phase. This discrepancy in experimental reports may be attributable to XRD patterns of a *P*1 phase (or phase region) being indistinguishable from higher symmetry tetragonal-like phases.

The most common high-compression substrate used in depositing epitaxial BFO thin films is $YAlO_3$, with a lattice constant of roughly 3.7 Å; this substrate leads to either to the *P1*-C or *Cc*-C phases, depending on the variation with thermal expansion of the lattice constant of YAO and the location of the transition from *P1*-C to *Cc*-C stability, which at 0 K is ∼3.705 Å. Although a further increase in the $c/a$ ratio can be attained by deposition beyond 7.9% compressive epitaxial strain in the true-tetragonal *P4mm*-C phase, no known experimental depositions of single-phase films in this region have been reported.

The change in the iron magnetic moment with epitaxial strain is shown in Fig. 3(a). The variation by >1% in the moment magnitude over the range of considered strain justifies the consideration of non-uniform moments in Eqs. (2)–(5). Of note is the discrepancy between the IP strain of 0%, indicating the IP lattice constant associated with the global minimum in the energy of the *Cc*-G phase, and the IP tensile strain of approximately 2%, indicating the global maximum in the iron magnetic moment. The magnetic moment of the B-site cation in a BXO system is predominately determined by the comparative degree to which spin-up and spin-down electronic states associate with the B-site cation. A necessary consideration in this regard is the strength of superexchange between 3d electronic states on the B-site cation and the 2p electronic states on intervening oxygen anions. While a separate analysis would be necessary to ascertain the precise basis in bonding theory for the variation in the magnetic moment under epitaxial strain, reasonable interference may be made that necessary considerations will include the twofold greater multiplicity of IP Fe–O bonds compared to OP bonds, the dependence of absolute superexchange on an exact 180° bond angle associated with each set of first-neighboring Fe–Fe pairs with an intervening oxygen, and the

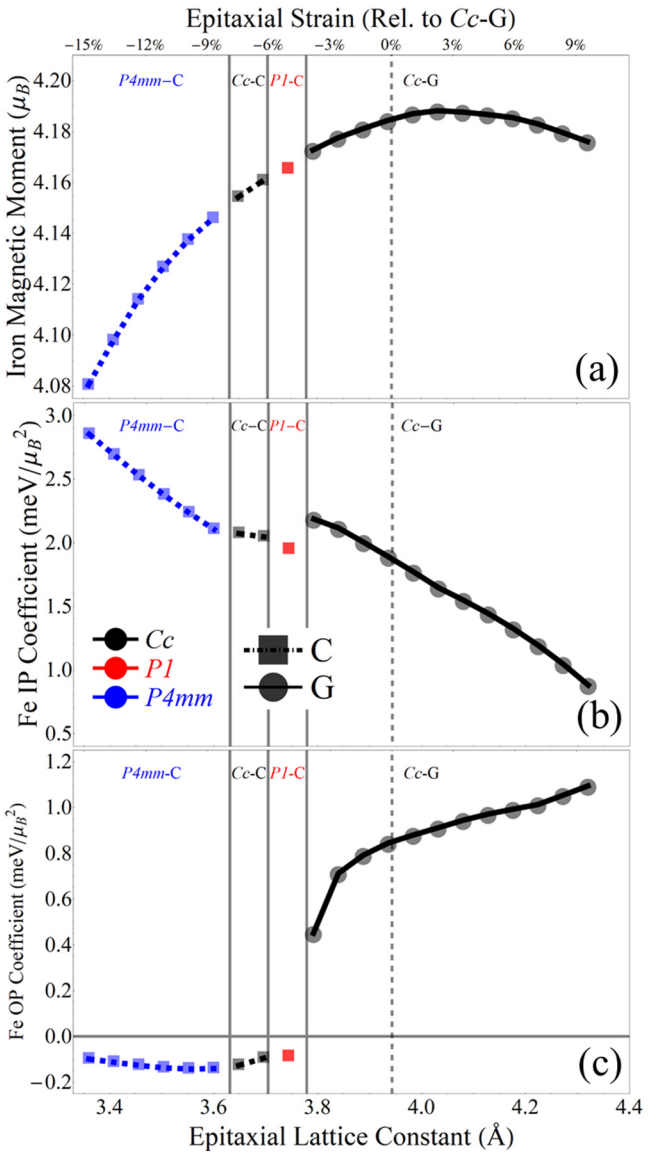


**FIG. 3.** (a) Magnetic moment of Fe ions, (b) in-plane magnetic coupling coefficient $J_{\parallel}$, and (c) out-of-plane coupling coefficient $J_{\perp}$ in stable phases of $BiFeO_3$, as a function of epitaxial lattice constant.

diminished correlation between spin-up and spin-down states on adjacent sites as interatomic spacing increases.[19]

The magnitude of the moments of all iron cations in the *Cc*-G phase at all values of epitaxial strain in this work is uniform throughout the entire 2 × 2 × 2 supercell. In the T-like *P1*-C, *Cc*-C, and *P4mm*-C phases, iron magnetic moments have one of two slightly different magnitudes distributed among Fe–Fe first-neighbor pairs such that all products of moments have equal magnitude for a given supercell. For these T-like phases, the reported moment magnitude in Fig. 3(a) is given as the square root of the magnitude of these products.

The reason for the sole presence of G-type and C-type magnetic orders in the BFO system across the entire strain range, with no transitions to A- or F-type order, is explained by the variation in IP magnetic coupling coefficient between adjacent iron cations with epitaxial strain, as illustrated in Fig. 3(b). Because the IP coefficient, $J_{\parallel}$, varies fairly linearly with IP lattice constant, the trend may be extrapolated to predict a sign reversal around 19% tensile epitaxial strain, beyond which point A-type order may be stable, barring any phase transitions or other discontinuous variations in structure.

The strong discontinuous decrease in magnitude and sign reversal of the OP coupling coefficient, shown in Fig. 3(c), is clearly associated with structural discontinuities around the 4.2% strain transition and the sudden drop in coordination (see Fig. 1 in the supplementary material) from 6 to 5. This decrease in coordination reflects an increase in one Fe–O interatomic spacing from 2–2.5 Å to 3–3.5 Å. The Fe–O atomic pair associated with this increase in spacing is uniform among all iron sites in a given BFO supercell. As such, the polarity of each $FeO_5$ polyhedra in T-like BFO is in constructive alignment. The opposing case in which adjacent polyhedra have anti-aligned polarities is definitively found in this work to be energetically unstable compared to the aligned case. The decrease in coordination from 6 to 5 is one factor underlying the dramatic increase in spontaneous OP polarization in the T-like phases of BFO. The basis in the superexchange effect for magnetic correlation in the BFO system explains why so long as both Fe–O bonds along the [001] crystallographic axis remain within a reasonable threshold for proper identification as chemical "bonds," anti-alignment of moments along this direction would be enforced.

Our prediction of ∼4.2% compressive strain, or an IP value of 3.79 Å, for the transition between G- and C-type order in BFO is similar to the values quoted in various parts of the literature for this transition, which range from 3.78 to 3.90 Å.[13,14] These prior works demonstrate that the sign on a coupling coefficient, including the values of strain where this coupling coefficient is zero, can be determined directly using the difference in energy of the various magnetic orders. Our work considers as well the variation in the magnetic moment with IP strain. This is necessary in order for the predicted values of the coupling coefficients to carry quantitative physical meaning as an assessment of the strength of magnetic coupling along each pair of neighboring B-site cations with an intervening oxygen anion. The results found herein are consistent with a Heisenberg-like model for the coupling between moments across first-neighboring Fe–Fe pairs only, with zero coupling coefficients between second or higher orders of Fe–Fe neighbors.

### B. Phase stability and magnetic properties of $BiCrO_3$

The BCO system is found to be stable in a *Cc*-G region of stability very similar to that found in BFO, even coinciding with an *R3c* phase at its local energy minimum. However, as shown in Fig. 4, this phase is not the globally lowest energy phase for BCO. Instead, one of a series of orthorhombic phases is the lowest energy, such that the *Cc*-G phase is only stable under tensile strain. The limited experimental investigations of BCO under epitaxial

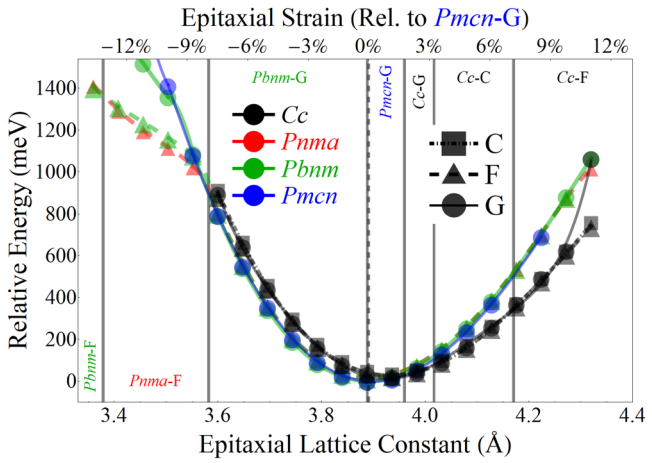


**FIG. 4.** Energetic stability of $BiCrO_3$ by space group and magnetic order, with strain referenced to the in-plane lattice constant ($a^* = 3.891$ Å) associated with the global minimum in the energy of the *Pmcn*-G phase.

strain typically use an $SrTiO_3$ substrate (3.90–3.95 Å lattice constant) and find pseudomonoclinic phase stability. Our results predict that the stable phase for an STO substrate is actually orthorhombic and is under slight tensile strain.[10]

The orthorhombic phases are quite energetically similar over the range of considered compressive strain, having energy differences between space groups as small as $10^{-5}$ eV/f.u. and differences between magnetic orders of the same space group as small as $10^{-6}$ eV/f.u. This similarity is finally broken beyond 7.9% compressive strain, at which point tetragonal-like phases become stable in the BCO system. These T-like phases, like those in BFO, exhibit lower B-site coordination than the corresponding R-like phases. An analysis of the Cr–O interatomic spacings (see Fig. 2 in supplementary material) indicates that half of the chromium cations in T-like BCO are coordinated with four oxygen anions, while half remain coordinated with six anions. This decrease in coordination is symmetric about the Cr–O pairs aligned with the OP crystallographic axis, with the two Cr–O pairs on four-coordinated sites increasing to an interatomic spacing of 3.0–3.5 Å, while the pairs on six-coordinated sites remaining bonded with an interatomic spacing of 2.0–2.5 Å. Whereas all of the BFO $FeO_5$ polyhedra in the T-like phases have significant polarities which constructively align, the BCO $CrO_4$ and $CrO_6$ polyhedra both have negligible polarities. Based on this, the ionic contribution to spontaneous polarization in "super-tetragonal" BCO will be far smaller than the corresponding contribution in super-tetragonal phases of BFO, though there may yet exist substantive electronic contributions.

The BCO system exhibits a dramatic discontinuity in the magnetic moment of certain chromium sites across the transition from the R-like *Pbnm*-G to the super-tetragonal *Pmcn*-F phase, as shown in Fig. 5(a). The chromium sites that remain octahedrally (CN = 6) coordinated have fairly continuous moments falling in the 2.95–3.10 $\mu_B$ range, whereas certain of the fourfold coordinated sites have dramatically larger moments, in the range of 3.25–3.75 $\mu_B$. Somewhat oddly, this dramatic dependence of the magnetic moment on coordination is largely removed in the *Pnma*-F phase, in which the difference in moments between the sites of each coordination environment reduces to roughly 0.05 $\mu_B$. However, whereas the *Pbnm*-F system exhibits uniform magnetic moments (within 0.001 $\mu_B$) on all chromium sites of a given coordination environment, the *Pnma*-F moments f chromium sites of a given coordination environment are not uniform. In this phase, the variance of moments among chromium sites of the same coordination is roughly $\pm 0.005\mu_B$.

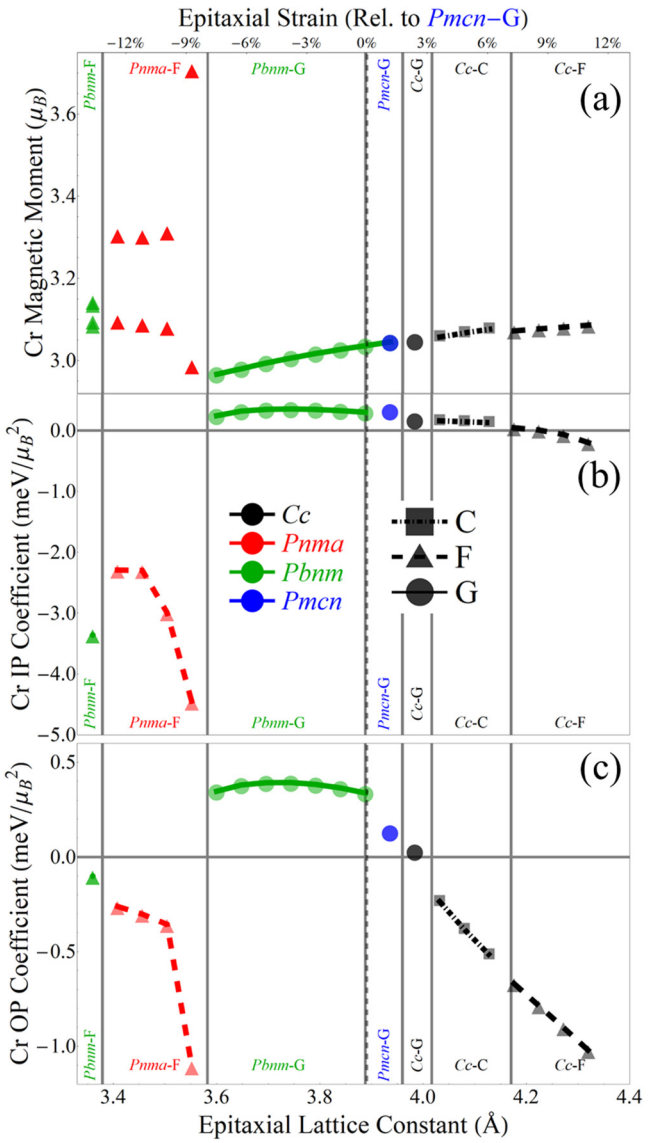


**FIG. 5.** (a) Magnetic moment of Cr ions, (b) in-plane magnetic coupling coefficient $J_{\parallel}$, and (c) out-of-plane coupling coefficient $J_{\perp}$ in stable phases of $BiCrO_3$, as a function of epitaxial lattice constant.

Figures 5(b) and 5(c) are consistent as well with high variation in coordination environment within the tetragonal-like phases. The region of intermediate C-type stability from 3.2% to 7.2% tensile epitaxial strain is possible because of the high continuity of structural order under tension in BCO. The absence of similar continuity across the R-like to T-like transition supports the direct transition from G- to F-type order, with no predicted intermediate region of A- or C-type order under compression. While our data are sufficient only to directly predict that the transition from G-type to F-type order in the BCO system occurs at some value between 7.5% and 8.7% compressive strain, the energetic continuity on either side of the predicted transition from *Pbnm*-G to *Pnma*-F at 7.9% strain and structural discontinuities associated with this transition are strongly consistent with attribution of a simultaneous reversal in sign of IP and OP coupling coefficients precisely at 7.9% strain with no intermediate region of A- or C-type stability.

The non-equivalence of coordination environment and magnetic moment of chromium sites suggests the possibility of the breakdown in the assumption of first nearest-neighbor only coupling coefficients. The distribution of fourfold and sixfold coordinated chromium sites suggests that in the *Pnma*-F phase, IP coupling is no longer first-neighbor only, while OP coupling remains first-neighbor only. In the *Pbnm*-F phase, all coupling is no longer first-neighbor only. However, coupling coefficients are still calculated and reported with consideration only of first-neighbor coupling. For the *Pnma*-F and *Pbnm*-F phases, the magnitude of the coupling coefficients should not be considered as having a quantitative value. However, the prediction of a transition from G- to F-type (full AFM to full FM) order at 7.9% compressive strain is quantitatively valid because this transition is based directly on relative energies.

The prediction of a region of C-type stability under tension is predicated on a separation of the epitaxial strains at which the IP and OP coupling coefficients reverse sign. The corresponding transitions under compression occur at the same 7.9% value of strain, such that there is no intermediate region of A- or C-type order between the region of *Pbnm*-G and *Pnma*-F phase stability. Under tension, the BCO structural order remains highly continuous with no dramatic changes in the chromium site coordination environment. Analysis of the Cr–O bond lengths in BCO under tensile strain (see Fig. 2 in the supplementary material) reveals that elements of orthorhombic symmetry remain in *Cc* monoclinic BCO, with Cr–O bond lengths falling into three pairs or equal-length bonds aligned along each of the three nearly orthogonal crystallographic axes.

## IV. CONCLUSIONS

Our investigation has established the range of chemical phases, which may be stable in the $BiFeO_3$ and $BiCrO_3$ systems under a large range of epitaxial strain, considering first-neighbor magnetic coupling and order. These computational predictions for the BFO system are entirely consistent with prior experimental results indicating an "R-like" to "T-like" transition in phase stability at 4.2% compressive epitaxial strain, including the result that this space group transition coincides exactly with a transition from G-type to C-type magnetic order. These assessments of space group and magnetic order are extended to the BCO system as well, demonstrating a transition to a "super-tetragonal" phase and discontinuous variation in the magnetic moment and coupling at 7.9% compressive strain. In addition, the BCO system may be stabilized in C-, F-, or G-type orders under accessible states of epitaxial strain. These results provide quantitative predictions of the atomic coordination environment and the magnetic behavior to be expected of two predominant bismuth-based perovskites over a range of epitaxial strain covering all currently known experimentally investigated cubic substrates for depositing perovskite thin films.

## SUPPLEMENTARY MATERIAL

See the supplementary material for a comparison of the general results of phase stability in the BFO system determined in this work to an array of relevant predictions in the extant literature, illustrations of the dependence on IP strain of interatomic spacing between the B-site cation and oxygen anions in each BXO system, and finally a tabulation of the supercell lattice constants associated with the minimum in the energy of each phase, which was found in this work to be the lowest energy for some range of IP strain in each BXO system.

## ACKNOWLEDGMENTS

M.R.W. was supported by a CoorsTek Research Fellowship through the Colorado School of Mines Foundation. G.L.B. and C.V.C. were supported in part by the National Science Foundation (NSF) through Grant No. DMR-1555015 and Grant No. DMREF-1629026, respectively.

## DATA AVAILABILITY

The data that support the findings of this study are available from the corresponding author upon reasonable request.

## REFERENCES

[1]A. A. Belik, "Polar and nonpolar phases of $BiMO_3$: A review," J. Solid State Chem. **195**, 32–40 (2012).
[2]K. Y. Yun, D. Ricinschi, T. Kanashima, M. Noda, and M. Okuyama, "Giant ferroelectric polarization beyond 150 $\mu C/cm^2$ in $BiFeO_3$ thin film," Jpn. J. Appl. Phys. **43**, L647–L648 (2004).
[3]R. Seshadri and N. A. Hill, "Visualizing the role of Bi 6s "lone pairs" in the off-center distortion in ferromagnetic $BiMnO_3$," Chem. Mater. **13**, 2892–2899 (2001).
[4]L. M. Volkova and D. V. Marinin, "Magnetoelectric ordering of $BiFeO_3$ from the perspective of crystal chemistry," J. Superconduct. Novel Magn. **24**, 2161–2177 (2011).
[5]A. A. Belik, S. Iikubo, K. Kodama, N. Igawa, S. Shamoto, and E. Takayama-Muromachi, "Neutron powder diffraction study on the crystal and magnetic structures of $BiCrO_3$," Chem. Mater. **20**, 3765–3769 (2008).
[6]N. A. Hill and K. M. Rabe, "First-principles investigation of ferromagnetism and ferroelectricity in bismuth manganite," Phys. Rev. B **59**, 8759–8769 (1999).
[7]G. A. Smolenskiĭ and I. E. Chupis, "Ferroelectromagnets," Sov. Phys. Usp. **25**, 475–493 (1982).
[8]A. A. Belik, S. Iikubo, K. Kodama, N. Igawa, S.-i. Shamoto, S. Niitaka, M. Azuma, Y. Shimakawa, M. Takano, F. Izumi, and E. Takayama-Muromachi, "Neutron powder diffraction study on the crystal and magnetic structures of $BiCoO_3$," Chem. Mater. **18**, 798–803 (2006).

[9]S. Ishiwata, M. Azuma, M. Takano, E. Nishibori, M. Takata, M. Sakata, and K. Kato, "High pressure synthesis, crystal structure and physical properties of a new Ni(II) perovskite $BiNiO_3$," J. Mater. Chem. **12**, 3733–3737 (2002).
[10]V. Kannan, M. Arredondo, F. Johann, D. Hesse, C. Labrugere, M. Maglione, and I. Vrejoiu, "Strain dependent microstructural modifications of $BiCrO_3$ epitaxial thin films," Thin Solid Films **545**, 130–139 (2013).
[11]P. Baettig, C. Ederer, and N. A. Spaldin, "First principles study of the multiferroics $BiFeO_3$, $Bi_2FeCrO_6$, and $BiCrO_3$," Phys. Rev. B **72**, 214105 (2005).
[12]M. R. Walden, C. V. Ciobanu, and G. L. Brennecka, "Stability of epitaxial $BiXO_3$ phases by density-functional theory," APL Mater. **8**, 081106 (2020).
[13]H.-C. Ding and C.-G. Duan, "Electric-field control of magnetic ordering in the tetragonal-like $BiFeO_3$," Europhys. Lett. **97**, 057007 (2012).
[14]C. Escorihuela-Sayalero, O. Diéguez, and J. Íñiguez, "Strain engineering magnetic frustration in perovskite oxide thin films," Phys. Rev. Lett. **109**, 247202 (2012).
[15]A. J. Hatt, N. A. Spaldin, and C. Ederer, "Strain-induced isosymmetric phase transition in $BiFeO_3$," Phys. Rev. B **81**, 054109 (2010).
[16]C.-S. Woo, J. H. Lee, K. Chu, B.-K. Jang, Y.-B. Kim, T. Y. Koo, P. Yang, Y. Qi, Z. Chen, L. Chen, H. C. Choi, J. H. Shim, and C.-H. Yang, "Suppression of mixed-phase areas in highly elongated $BiFeO_3$ substrates," Phys. Rev. B **86**, 054417 (2012).
[17]R. J. Zeches, M. D. Rossell, J. X. Zhang, A. J. Hatt, Q. He, C.-H. Yang, A. Kumar, C. H. Wang, A. Melville, C. Adamo, G. Sheng, Y.-H. Chu, J. F. Ihlefeld, R. Erni, C. Ederer, V. Gopalan, L. Q. Chen, D. G. Schlom, N. A. Spaldin, L. W. Martin, and R. Ramesh, "A strain-driven morphotropic phase boundary in $BiFeO_3$," Science **326**, 977–980 (2009).
[18]J. C. Wojdeł and J. Íñiguez, "*Ab initio* indications for giant magnetoelectric effects driven by structural softness," Phys. Rev. Lett. **105**, 037208 (2010).
[19]T. Moriya, "Anisotropic superexchange interaction and weak ferromagnetism," Phys. Rev. **120**, 91–98 (1960).
[20]B. Dupé, I. C. Infante, G. Geneste, P.-E. Janolin, M. Bibes, A. Barthélémy, S. Lisenkov, L. Bellaiche, S. Ravy, and B. Dkhil, "Competing phases in $BiFeO_3$ thin films under compressive epitaxial strain," Phys. Rev. B **81**, 144128 (2010).
[21]C. W. Huang, Y. H. Chu, Z. H. Chen, J. Wang, T. Sritharan, Q. He, R. Ramesh, and L. Chen, "Strain-driven phase transitions and associated dielectric/piezoelectric anomalies in $BiFeO_3$ thin films," Appl. Phys. Lett. **97**, 152901 (2010).
[22]J. X. Zhang, Q. He, M. Trassin, W. Luo, D. Yi, M. D. Rossell, P. Yu, L. You, C. H. Wang, C. Y. Kuo, J. T. Heron, Z. Hu, R. J. Zeches, H. J. Lin, A. Tanaka, C. T. Chen, L. H. Tjeng, Y.-H. Chu, and R. Ramesh, "Microscopic origin of the giant ferroelectric polarization in tetragonal-like $BiFeO_3$," Phys. Rev. Lett. **107**, 147602 (2011).
[23]N. Dix, J. Fontcuberta, F. Sánchez, P. Jadhav, O. Chaix-Pluchery, M. Varela, and J. Kreisel, "A phase transition close to room temperature in $BiFeO_3$ thin films," J. Phys.: Condens. Matter **23**, 342202 (2011).
[24]H. Liu, P. Yang, K. Yao, K. P. Ong, P. Wu, and J. Wang, "Origin of a tetragonal $BiFeO_3$ phase with a giant c/a ratio on $SrTiO_3$ substrates," Adv. Funct. Mater. **22**, 937–942 (2012).
[25]H. Béa, B. Dupé, S. Fusil, R. Mattana, E. Jacquet, B. Warot-Fonrose, F. Wilhelm, A. Rogalev, S. Petit, V. Cros, A. Anane, F. Petroff, K. Bouzehouane, G. Geneste, B. Dkhil, S. Lisenkov, I. Ponomareva, L. Bellaiche, M. Bibes, and A. Barthélémy, "Evidence for room-temperature multiferroicity in a compound with a giant axial ratio," Phys. Rev. Lett. **102**, 217603 (2009).
[26]J. F. Ihlefeld, N. J. Podraza, Z. K. Liu, R. C. Rai, X. Xu, T. Heeg, Y. B. Chen, J. Li, R. W. Collins, J. L. Musfeldt, X. Q. Pan, J. Schubert, R. Ramesh, and D. G. Schlom, "Optical band gap of $BiFeO_3$ grown by molecular-beam epitaxy," Appl. Phys. Lett. **92**, 142908 (2008).
[27]F. Zavaliche, S. Y. Yang, T. Zhao, Y. H. Chu, M. P. Cruz, C. B. Eom, and R. Ramesh, "Multiferroic $BiFeO_3$ films: Domain structure and polarization dynamics," Phase Trans. **79**, 991–1017 (2006).
[28]G. Kresse and J. Hafner, "*Ab initio* molecular dynamics for liquid metals," Phys. Rev. B **47**, 558–561 (1993).
[29]G. Kresse and J. Hafner, "*Ab initio* molecular-dynamics simulation of the liquid-metalamorphous-semiconductor transition in germanium," Phys. Rev. B **49**, 14251–14269 (1994).
[30]G. Kresse and J. Furthmüller, "Efficiency of *ab initio* total energy calculations for metals and semiconductors using a plane-wave basis set," Comput. Mater. Sci. **6**, 15–50 (1996).
[31]G. Kresse and J. Furthmüller, "Efficient iterative schemes for *ab initio* total-energy calculations using a plane-wave basis set," Phys. Rev. B **54**, 11169–11186 (1996).
[32]J. P. Perdew, J. A. Chevary, S. H. Vosko, K. A. Jackson, M. R. Pederson, D. J. Singh, and C. Fiolhais, "Atoms, molecules, solids, and surfaces: Applications of the generalized gradient approximation for exchange and correlation," Phys. Rev. B **46**, 6671–6687 (1992).
[33]J. P. Perdew, K. Burke, and M. Ernzerhof, "Generalized gradient approximation made simple," Phys. Rev. Lett. **77**, 3865–3868 (1996).
[34]J. P. Perdew, K. Burke, and M. Ernzerhof, "Erratum: Generalized gradient approximation made simple," Phys. Rev. Lett. **78**, 1396 (1997).
[35]G. I. Csonka, J. P. Perdew, A. Ruzsinszky, P. H. Philipsen, S. Lebègue, J. Paier, O. A. Vydrov, and J. G. Ángyán, "Assessing the performance of recent density functionals for bulk solids," Phys. Rev. B **79**, 155107 (2009).
[36]G. Kresse and D. Joubert, "From ultrasoft pseudopotentials to the projector augmented-wave method," Phys. Rev. B **59**, 1758–1775 (1999).
[37]S. L. Dudarev, G. A. Botton, S. Y. Savrasov, C. J. Humphreys, and A. P. Sutton, "Electron-energy-loss spectra and the structural stability of nickel oxide: An LSDA+U study," Phys. Rev. B **57**, 1505–1509 (1998).
[38]V. I. Anisimov, A. I. Poteryaev, M. A. Korotin, A. O. Anokhin, and G. Kotliar, "First-principles calculations of the electronic structure and spectra of strongly correlated systems: Dynamical mean-field theory," J. Phys.: Condens. Matter **9**, 7359–7367 (1997).
[39]M. Cococcioni and S. de Gironcoli, "Linear response approach to the calculation of the effective interaction parameters in the LDA+U method," Phys. Rev. B **71**, 035105 (2005).
[40]M. B. Kanoun, S. Goumri-Said, U. Schwingenschlögl, and A. Manchon, Magnetism in Sc-doped ZnO with zinc vacancies: A hybrid density functional and GGA + U approaches," Chem. Phys. Lett. **532**, 96–99 (2012).
[41]M. Yashima and R. O. Suzuki, "Electronic structure and magnetic properties of monoclinic β-$Cu_2V_2O_7$: A GGA+U study," Phys. Rev. B **79**, 125201 (2009).
[42]D. Stoeffler and C. Etz, "*Ab initio* electronic structure and magnetism in $Sr_2XMoO_6$ (X = Fe or Co) double perovskite systems: A GGA and GGA+U comparative study," J. Phys.: Condens. Matter **18**, 11291–11300 (2006).
[43]P. E. Blöchl, "Projector augmented-wave method," Phys. Rev. B **50**, 17953–17979 (1994).
[44]J. T. Zhang, C. Ji, J. L. Wang, W. S. Xia, X. M. Lu, and J. S. Zhu, "Stabilization of *E*-type magnetic order caused by epitaxial strain in perovskite manganites," Phys. Rev. B **97**, 085124 (2018).
[45]Z. Chen, S. Prosandeev, Z. L. Luo, W. Ren, Y. Qi, C. W. Huang, L. You, C. Gao, I. A. Kornev, T. Wu, J. Wang, P. Yang, T. Sritharan, L. Bellaiche, and L. Chen, "Coexistence of ferroelectric triclinic phases in highly strained $BiFeO_3$ films," Phys. Rev. B **84**, 094116 (2011).